Available online at www.sciencedirect.com
SCIENCE DIRECT®
International Journal of Thermal Sciences 43 (2004) 939–950
International Journal of Thermal Sciences
www.elsevier.com/locate/ijts

Transient combined radiation and conduction heat transfer in fibrous media with temperature and flux boundary conditions

Fatmir Asllanaj [a], Gérard Jeandel [a], Jean Rodolphe Roche [b], David Lacroix [a]

[a] *LEMTA, faculté des sciences et techniques, BP 239, 54506 Vandoeuvre-les-Nancy, France*
[b] *IECN, faculté des sciences et techniques, BP 239, 54506 Vandoeuvre-les-Nancy, France*

Received 27 September 2003; received in revised form 4 February 2004; accepted 27 February 2004

Available online 9 June 2004

Abstract

Transient radiative and conductive heat transfer in a fibrous medium with anisotropic optical properties is investigated. Two different kinds of boundary conditions are treated: when the temperatures imposed on the boundaries vary with time and when the medium is subject to a radiation source which varies with time. A one dimensional case is considered. The non-linear transient Heat Conduction Equation is solved using the Kirchhoff transformation associated with a P^2 finite elements method using a non-uniform spatial mesh. The Radiative Transfer Equation is solved using a direct method which is analytical in space whereas the spectral scattering and absorption coefficients as well as the phase function are determined using the Mie theory. This procedure is applied on the whole time domain. Finally, a realistic application to a fibrous insulation composed of silica fibers is treated numerically.

Keywords: Transient coupled radiative–conductive heat transfer; Finite elements method; Kirchhoff transformation; Semi-transparent; Fibrous media

1. Introduction

Beyond a certain temperature, the thermomechanical properties of insulating materials deteriorate and, moreover, phase changes can locally appear, which might produce asphyxiation or irreversible damage to persons. To prevent this, fibrous insulation materials must meet rigorous standards. Accordingly, the assessment of any insulating material under fire conditions requires evaluating the temperature field in the medium and its evolution with time. For this purpose, we have carried out a modelling of the coupled radiation and conduction heat transfer in transient state inside a semi-transparent plate, with a heat flux applied to one of the faces. The interest of such modelling is to allow optimisation of composition in order to satisfy the imposed criterion. The complete modelling of phenomena is delicate because materials containing silica cannot be considered as grey media and the radiative properties vary with the wavelength and the direction. Our study takes into account this complex radiative behaviour [1–7].

A survey of the literature on coupled radiation and conduction in semi-transparent media shows that, up to now, there exist rather few studies on the transient state and, that for the major part, the media considered are gray not scattering [8–11] or with an isotropic scattering [12–18]. Some authors consider however non-gray media and scattering [19], either isotropic [20], or anisotropic [21]. Moreover, problems corresponding to imposed temperatures on the boundaries have been largely modelled, but there exist rather few studies dealing with flux boundary conditions. In addition, note that in the quoted papers, fibrous media are practically not studied. However, the practical and economic stakes remain significant.

The two major modes of heat transfer in insulating materials that we will study are radiation and conduction. Previous studies about heat transfer through fibrous media [3,5] have shown that radiative heat transfer might constitute half of the total heat transfer, for a medium with a temperature ranging between 300 and 400 K. Moreover, transmission and reflection measurements in such media exhibit non-isotropic scattering properties. Steady state heat transfer by combined

E-mail addresses: Fatmir.Asllanaj@lemta.uhp-nancy.fr (F. Asllanaj), gerard.jeandel@lemta.uhp-nancy.fr (G. Jeandel), david.lacroix@lemta.uhp-nancy.fr (J.R. Roche), roche@iecn.u-nancy.fr (D. Lacroix).

1290-0729/$ – see front matter
doi:10.1016/j.ijthermalsci.2004.02.007

Nomenclature

c_p	specific heat capacity of the medium	$J \cdot kg^{-1} \cdot K^{-1}$	
E	medium thickness	m	
h	convective exchange coefficient	$W \cdot m^{-2} \cdot K^{-1}$	
I_λ	spectral radiation intensity	$W \cdot m^{-2} \cdot \mu m^{-1} \cdot sr^{-1}$	
$I_{b,\lambda}$	spectral black body intensity	$W \cdot m^{-2} \cdot \mu m^{-1} \cdot sr^{-1}$	
k	thermal conductivity of the medium	$mW \cdot m^{-1} \cdot K^{-1}$	
Q_t	total heat flux	$W \cdot m^{-2}$	
Q_c	conductive heat flux	$W \cdot m^{-2}$	
Q_r	total radiative heat flux	$W \cdot m^{-2}$	
S_r	radiative source term	$W \cdot m^{-3}$	
t	time	s	
T	temperature	K	
T_∞	surrounding temperature	K	
x	position	m	

Greek symbols

λ	wavelength	μm
μ	cosine of the polar angle	
ρ	density of the medium	$kg \cdot m^{-3}$
κ_λ	spectral absorption coefficient	m^{-1}
$\sigma_{s\lambda}$	spectral scattering coefficient	m^{-1}
β_λ	spectral extinction coefficient	m^{-1}
Φ_λ	spectral phase function	

Subscripts

0, E	boundaries
λ	spectral

radiation and conduction in a fibrous medium, limited by black surfaces with temperatures imposed, was already dealt with in references [3–5,22–25]. In the present work, we propose to extend this study by considering the transient state. First, we will consider as boundary conditions the temperatures imposed on the boundaries and, later, we will extend the study by including flux boundary conditions.

2. Theory and analysis

2.1. Physical model and mathematical formulation

We consider heat transfer in the transient state through a planar fibrous medium. The medium is assumed to be homogeneous, one-dimensional, and axisymetric with thickness E. To describe the radiation–conduction interaction inside a semi-transparent medium, two equations are necessary: the radiative transfer equation (RTE) and the energy conservation equation.

Lind and Greenberg [36] have shown that the interaction of the radiation with a fibre varies with the incoming angle. The studied medium is nonhomogenous and anisotropic: it is made of air and silica fibres randomly oriented in planes parallel to the boundaries. The Lorentz–Mie theory [5–7] makes it possible to determine the radiative properties of the homogeneous medium equivalent to the real medium. For the independent diffusion, one considers that the radiative properties of the medium are obtained from the radiative properties of each fibre (Fig. 3 in [5]). As detailed in our previous papers and in Fig. 1, the spectral variation of the radiative properties shows that the fibrous medium under consideration is clearly non-grey. Fig. 1 shows the distribution of radiative coefficients with the direction and the wavelength. In addition, this fibrous medium has strongly anisotropic radiative properties. Accordingly, the full set of radiative properties

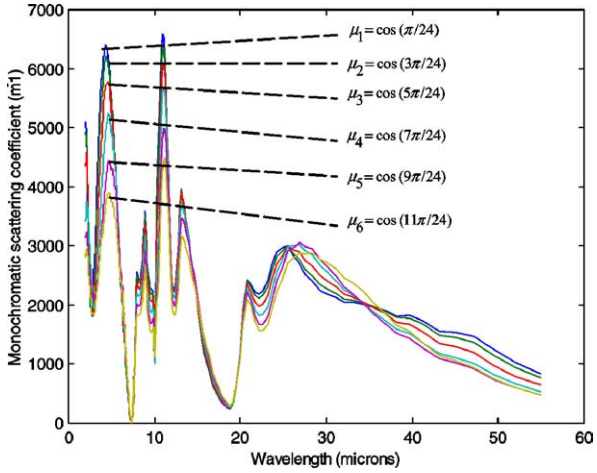

(a)

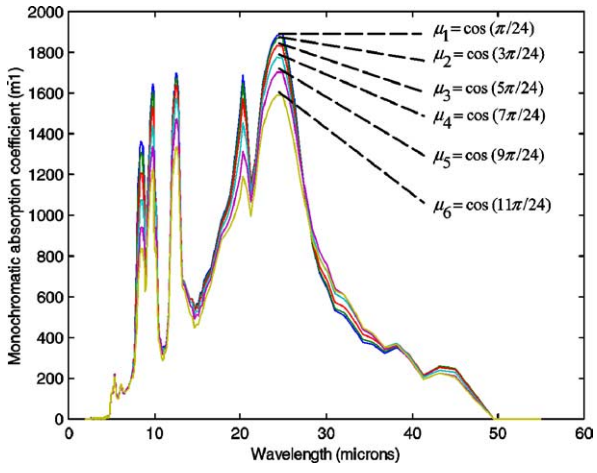

(b)

Fig. 1. (a) Variation of scattering coefficient with the direction and the wavelength. (b) Variation of absorption coefficient with the direction and the wavelength.

must be evaluated: the spectral absorption, scattering coefficients κ_λ, $\sigma_{s\lambda}$ and the spectral phase function Φ_λ. They are determined from the Mie theory [5–7].

2.1.1. The radiative transfer equation (RTE)

In our fibrous media and for the applications which we have to consider, the spectral radiation intensity $I_\lambda(x,\mu,t)$ is governed by the RTE [26], which is written for the wavelength λ, at the position x, in the direction μ and at time t as

$$\mu\frac{\partial I_\lambda(x,\mu,t)}{\partial x} = -\beta_\lambda(\mu)I_\lambda(x,\mu,t) + J_\lambda(x,\mu,t) \tag{1}$$

with

$$\beta_\lambda = \kappa_\lambda + \sigma_{s\lambda} \tag{2}$$

and

$$J_\lambda(x,\mu,t) = \kappa_\lambda(\mu)I_{b,\lambda}\big(T(x,t)\big) + \frac{1}{2}\int_{\mu'=-1}^{1}\sigma_{s\lambda}(\mu')\Phi_\lambda(\mu'\to\mu)I_\lambda(x,\mu',t)\,\mathrm{d}\mu' \tag{3}$$

for all $0 < x < E$, $t > 0$, $\mu \in [-1,1]\backslash\{0\}$, $\lambda > 0$. The coefficient c denotes the radiation propagation speed in the medium. The coefficient μ is the cosine of the polar angle between the directions of propagation and transfer. In Eq. (1), the terms on the right-hand side describe respectively the extinction phenomena, the internal emission and the intensity of the scattering in the μ direction. The function $I_{b,\lambda}(T)$ is the spectral intensity of black body emission at temperature T, given by Planck's law as:

$$I_{b,\lambda}(T) = \frac{C_1}{\lambda^5\cdot[\exp(C_2/(\lambda\cdot T))-1]} \tag{4}$$

where C_1 and C_2 are two constants of radiation given by:

$$C_1 = 1.19\times10^{-16}\ \mathrm{W\cdot m^2\cdot sr^{-1}} \quad \text{and}$$
$$C_2 = 1.4388\times10^{-2}\ \mathrm{m\cdot K}$$

The constant C_1 is the C_1 black body constant [27] for an index of refraction close to one. Our material is made of silica fibres and air with a preponderance of air. The silica density is equal to: $\rho_{\mathrm{glass}} = 2500\ \mathrm{kg\cdot m^{-3}}$ and our material density is equal to: $\rho = 20\ \mathrm{kg\cdot m^{-3}}$. Thus, we can assume, for our material, a refraction index close to one.

Eq. (4) gives access to the spectral radiation intensity at each point of the medium, in each direction and at any time. The total radiative heat flux is then given by:

$$Q_r(x,t) = 2\pi\int_{\lambda=0}^{\infty}\int_{\mu=-1}^{1} I_\lambda(x,\mu,t)\mu\,\mathrm{d}\mu\,\mathrm{d}\lambda \tag{5}$$

2.1.2. The energy equation

The transient temperature responses in the medium are the solutions of the non-linear energy equation which is written at the position x and at time t, according to:

$$\rho c_p\frac{\partial T}{\partial t}(x,t) - \frac{\partial}{\partial x}\left(k\big(T(x,t)\big)\frac{\partial T}{\partial x}(x,t)\right) = S_r(x,t) \tag{6}$$

for all $0 < x < E$ and $t > 0$. The coefficients ρ and c_p are the medium density and the medium specific heat capacity respectively. For our applications, they are constant and equal to $\rho = 20\ \mathrm{kg\cdot m^{-3}}$ and $c_p = 670\ \mathrm{J\cdot kg^{-1}\cdot K^{-1}}$.

The function $k(T)$ is the medium thermal conductivity which is temperature dependent. $k(T)$ is derived using the Langlais and Klarsfeld semi-empirical relation developed for insulations made of silica fibers. It is based on experimental data obtained from a guarded hot plate device (Saint Gobain Research Center [27]):

$$k(T) = 0.2572T^{0.81} + 0.0527\rho^{0.91}(1+0.0013T) \tag{7}$$

This relation corresponds to the heat transfer through the thickness of the insulator and takes into account the air and glass fiber conduction as well as the contacts between fibers. The validity range of this relation is for a temperature from approximately 273 to 1000 K.

Note that, we do not take into account any convective term. In our case, air movement between fibers that might induce convection is neglected.

Eq. (6) is coupled with the radiative transfer via the radiative source term:

$$S_r(x,t) = -\frac{\partial Q_r}{\partial x}(x,t) \tag{8}$$

where Q_r is given by relation (5). The conductive heat flux is defined by:

$$Q_c(x,t) = -k\big(T(x,t)\big)\frac{\partial T}{\partial x}(x,t) \tag{9}$$

The total heat flux is given by the sum of radiative and conductive heat fluxes:

$$Q_t = Q_r + Q_c \tag{10}$$

In steady state, the energy equation becomes:

$$\frac{\mathrm{d}Q_t}{\mathrm{d}x}(x) = 0 \tag{11}$$

We point out that the numerical method used to solve the coupled problem, that we will detail below, leads to a solution satisfying this condition, at the final time t_f at which the steady-state is reached (within a given tolerance).

2.1.3. Boundary conditions and initial condition

2.1.3.1. Temperature boundary conditions and initial condition. The first problem, corresponds to a system called: "guarded hot plates". The medium boundaries are black surfaces with imposed temperatures. Initially, the system is at a uniform temperature. The temperature of the front face—the hot face—is assumed to be raised abruptly following a given

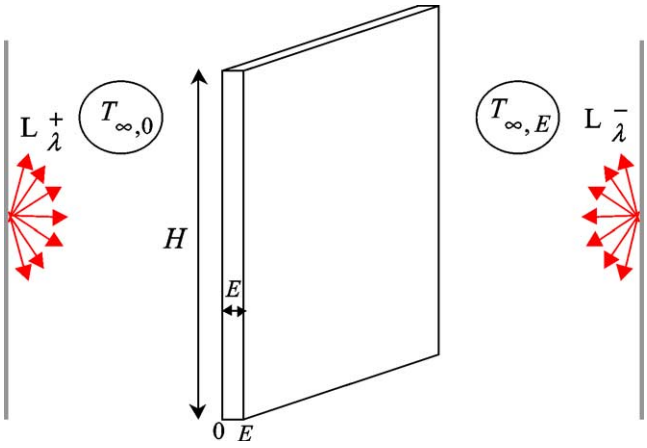

Fig. 2. Plane plate lit by two radiation sources on its two surfaces.

time evolution $f(t)$ to reach a constant value T_0. The cold face temperature $T(E,t)$ remains constant with time. Mathematically, the thermal boundary conditions are thus the following:

$$T(0,t) = f(t) \quad \text{and} \quad T(E,t) = T_E \quad \text{for } t > 0 \tag{12}$$

where f is a given function with $f(t) \to T_0$ and the radiative boundary conditions [26] are for $t \geqslant 0$:

$$\begin{aligned} &I_\lambda(0,\mu,t) = I_{b,\lambda}(f(t)) \quad \text{for } 0 < \mu \leqslant 1 \\ &I_\lambda(E,\mu,t) = I_{b,\lambda}(T_E) \quad \text{for } -1 \leqslant \mu < 0 \end{aligned} \tag{13}$$

As to the initial condition in the medium:

$$T(x,0) = T_E \quad \text{for } 0 \leqslant x \leqslant E \tag{14}$$

2.1.3.2. Flux boundary conditions and initial condition. The second problem corresponds to a sample lit by a radiation source. The sample is assumed to be a plane plate, vertically positioned in air with no motion (Fig. 2). The two faces $x = 0$ and $x = E$ are in contact with surrounding temperatures $T_{\infty,0}$ and $T_{\infty,E}$, respectively, and the superficial exchanges between wall and environment are characterised by convective exchange coefficients h_0 and h_E. Then, two different radiation sources of time-varying intensities are applied on the two faces respectively (Fig. 2). They are defined by:

- $L_\lambda^+(\mu,t)$ with $0 < \mu \leqslant 1$ and $t > 0$ for the front face (i.e., in $x = 0$);
- $L_\lambda^-(\mu,t)$ with $-1 \leqslant \mu < 0$ and $t > 0$ for the back face (i.e., in $x = E$).

In the case of an insulating materials, of a glass wool type, the silica fibers are stratified randomly, in more or less parallel planes between the medium boundaries (Fig. 3). Thus, we may consider the faces as being practically transparent, because the fiber density is very low and the probability of an incoming ray meeting a fiber in the plane of the interface is negligible compared to that crossing the air (Fig. 3). In this case, radiative boundary conditions are given by:

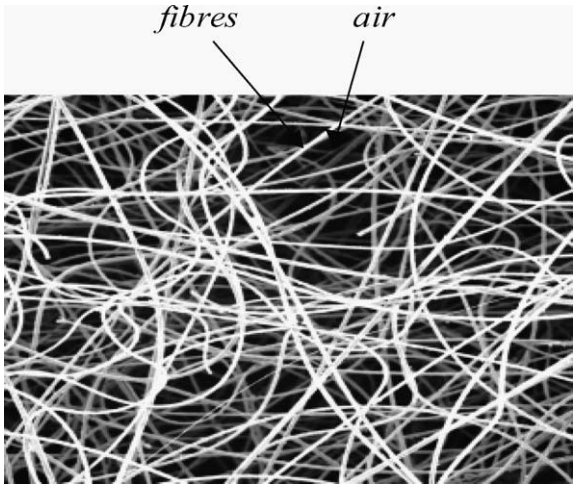

Fig. 3. Studied sample: insulator made of silica fibers.

$$\begin{aligned} &\text{at} \quad x = 0, \ I_\lambda(0,\mu,t) = L_\lambda^+(\mu,t) \\ &\qquad \text{for } 0 < \mu \leqslant 1, \ t > 0 \\ &\text{at} \quad x = E, \ I_\lambda(E,\mu,t) = L_\lambda^-(\mu,t) \\ &\qquad \text{for } -1 \leqslant \mu < 0, \ t > 0 \end{aligned} \tag{15}$$

With this assumption of purely transparent boundaries, thermal boundary conditions are:

$$\begin{aligned} &\text{at} \quad x = 0, \quad -k(T)\frac{\partial T}{\partial x} + h_0(T)(T - T_{\infty,0}) = 0 \\ &\text{at} \quad x = E, \quad k(T)\frac{\partial T}{\partial x} + h_E(T)(T - T_{\infty,E}) = 0 \end{aligned} \tag{16}$$

The expressions of convective exchange coefficients h_0 and h_E are given in the appendix. The initial condition is a constant temperature in the medium:

$$T(x,0) = T_E \quad \text{for } 0 \leqslant x \leqslant E \tag{17}$$

2.2. Method of solution of coupled heat transfer

The above two equations described in Section 2.1 define a strongly coupled system of non-linear partial derivate and integro differential equations, where the unknowns are the spectral radiation intensity and the temperature fields. There is no known analytical solution to these equations. The RTE will be solved by a direct method which is analytical in space. In this paper, the solution is achieved numerically using a discretization of the medium as well as of the direction and the time domains: the radiation intensity and the temperature fields are approximated at various points (nodes of the mesh), in various discrete directions for intensity and at various times.

Furthermore, if a fast temperature variation or a very intense radiation source is applied on one of the two faces of the medium, we first observe a very high temperature gradient near this face. This implies that, in this kind of

problem, the zone with strong temperature gradient requires a refined treatment. But, for computing time reasons, it is not appropriate to use a uniformly fine mesh everywhere in the medium. Moreover, in the transient case, the evolution of temperature can be very stiff at the beginning, which implies that the time step should also be adapted. The finite elements method is well adapted to non-uniform spatial meshes and makes it possible to obtain good accuracy. Thus, this method will be used to solve the energy equation. The coupled system of equations will be solved by iteration versus time. These different methods of solution will be explained further.

2.2.1. Solution of the radiative transfer equation

The RTE given by relation (4) is "quasi-stationary". In other words, time occurs in the equation only through the temperature field. The time variable is considered merely as a parameter. The dependence of the spectral radiation intensity on time is then implicit through the temperature. The transient evolution of the temperature field is described by the energy equation given by relation (6). Hence, for a given temperature field and at a given time, the solution of RTE in the transient-state is the same as in the steady-state. Thus, the steady state method given by [23] is used to solve the RTE. This method uses a multi-flux model. An angular discretization technique (discrete ordinates approximation) is applied in order to express the RTE in an inhomogeneous system of linear differential equations associated with Dirichlet boundary conditions. This system is solved by a direct method (matrix exponential method), after diagonalizing the medium characteristic matrix, which makes it possible to circumvent the numerical instability problem. This method is efficient in terms of computational times and the solution is analytical in space (see [22,23]).

2.2.2. Solution of the energy equation

A spatial semi-discretization of the energy equation is obtained by the finite elements method. To solve this equation, the radiative source term S_r is assumed to be given.

The energy equation is non-linear due to the temperature-dependence of the thermal conductivity. In order to "linearize" the problem, the Kirchhoff transformation is introduced [28,29]. It is a transformation of the dependent variable and is a classical tool for solving non-linear partial differential equations. It is defined by:

$$\Psi_c(u) = \int_0^u k(s)\,\mathrm{d}s$$

Applying this transformation to the energy equation, we obtain a new formulation of the equation:

$$\rho c_p \frac{\partial T}{\partial t}(x,t) - \frac{\partial^2(\Psi_c \circ T)}{\partial x^2}(x,t) = S_r(x,t) \quad \forall (x,t) \in (0,E)\times(0,t_f] \tag{18}$$

Applying the Kirchhoff transformation to the thermal boundary conditions given by (16), we obtain

$$-\frac{\partial(\Psi_c \circ T)}{\partial x}(0,t) + h_0\big(T(0,t)\big)\cdot\big(T(0,t) - T_{\infty,0}(t)\big) = 0 \quad \forall t \in (0,t_f]$$
$$\frac{\partial(\Psi_c \circ T)}{\partial x}(E,t) + h_E\big(T(E,t)\big)\cdot\big(T(E,t) - T_{\infty,E}(t)\big) = 0 \quad \forall t \in (0,t_f] \tag{19}$$

The spatial semi-discretization by the finite elements method uses the variational formulation and the Galerkin approximation. This technique is classical and many works refer to it. See, for instance, the following books [30,31].

The following scalar product is introduced:

$$(u,v) = \int_0^E u(x)\cdot v(x)\,\mathrm{d}x$$

The functions φ_i, $0 \leqslant i \leqslant N+1$ denote the basis functions. Taking into account that the expression of conductive heat flux given by (9) uses the first spatial derivative of the temperature, the basic Lagrange quadratic functions are used for the basis functions. Thus, we will have piecewise linear functions for the conductive heat flux. The description of these functions can be found in [31].

For the problem relating to temperature boundary conditions, we obtain the following differential system [22]:

$$\frac{\mathrm{d}\boldsymbol{T}(t)}{\mathrm{d}t} = \frac{1}{\rho c_p}\cdot[M]^{-1} \times \big\{-[R]\cdot\Psi_c\big(\boldsymbol{T}(t)\big) + \boldsymbol{S}_r(t) - \rho\cdot c_p\cdot f'(t)\cdot\boldsymbol{M}^0 - \Psi_c\big(f(t)\big)\cdot\boldsymbol{R}^0 - \Psi_c(T_E)\cdot\boldsymbol{R}^E\big\} \quad \forall t \in (0,t_f] \tag{20}$$

with the initial condition: $T_j(0) = T_E$, $\forall 1 \leqslant j \leqslant N$, where

- $\boldsymbol{T}(t)$ is the vector of components $T_j(t)$, $1 \leqslant j \leqslant N$;
- $\Psi_c(\boldsymbol{T}(t))$ is the vector of components $\Psi_c(T_j(t))$, $1 \leqslant j \leqslant N$;
- $[M]$ is the square matrix of coefficients $[M]_{i,j} = (\varphi_i, \varphi_j)$, $1 \leqslant i, j \leqslant N$;
- $[R]$ is the square matrix of coefficients $[R]_{i,j} = (\varphi_i', \varphi_j')$, $1 \leqslant i, j \leqslant N$;
- $\boldsymbol{S}_r(t)$ is the vector of which the ith component is $(\boldsymbol{S}_r)_i(t) = \big(S_r(\cdot,t), \varphi_i\big)$, $\quad 1 \leqslant i \leqslant N$
- $\boldsymbol{M}^0$ is the vector of components $\boldsymbol{M}_i^0 = (\varphi_0, \varphi_i)$, $1 \leqslant i \leqslant N$;
- $\boldsymbol{R}^0$ is the vector of components $\boldsymbol{R}_i^0 = (\varphi_0', \varphi_i')$, $1 \leqslant i \leqslant N$;
- $\boldsymbol{R}^E$ is the vector of components $\boldsymbol{R}_i^E = (\varphi_{N+1}', \varphi_i')$, $1 \leqslant i \leqslant N$.

For the problem relating to flux boundary conditions, we obtain the following differential system [22]:

$$\frac{\mathrm{d}\boldsymbol{T}(t)}{\mathrm{d}t} = \frac{1}{\rho c_p} \cdot [M]^{-1} \cdot \left\{ -[R] \cdot \Psi_c\big(\boldsymbol{T}(t)\big) + \boldsymbol{S}_r(t) - \big[H\big(\boldsymbol{T}(t)\big)\big] \cdot \big(\boldsymbol{T}(t) - \boldsymbol{T}_\infty(t)\big) \right\} \quad \forall t \in (0, t_f] \tag{21}$$

with the initial condition $T_j(0) = T_E$, $\forall 0 \leqslant j \leqslant N+1$, where

- $\boldsymbol{T}(t)$ is the vector of components $T_j(t)$, $0 \leqslant j \leqslant N+1$;
- $\Psi_c(\boldsymbol{T}(t))$ is the vector of components $\Psi_c(T_j(t))$, $0 \leqslant j \leqslant N+1$;
- $[M]$ is the square matrix of coefficients

  $[M]_{i,j} = (\varphi_i, \varphi_j), \quad 0 \leqslant i, j \leqslant N+1$
- $[R]$ is the square matrix of coefficients

  $[R]_{i,j} = \big(\varphi_i', \varphi_j'\big), \quad 0 \leqslant i, j \leqslant N+1$
- $\boldsymbol{S}_r(t)$ is the vector which the ith component is

  $(\boldsymbol{S}_r)_i(t) = \big(S_r(\cdot, t), \varphi_i\big), \quad 1 \leqslant i \leqslant N$
- $\boldsymbol{T}_\infty(t)$ is the vector of components

$$(\boldsymbol{T}_\infty)_j(t) = \begin{cases} T_{\infty,0}(t) & \text{if } j = 0 \\ 0 & \text{if } 1 \leqslant j \leqslant N \\ T_{\infty,E}(t) & \text{if } j = N+1 \end{cases}$$

- $[H(\boldsymbol{T}(t))]$ is the square matrix of coefficients

$$\big[H\big(\boldsymbol{T}(t)\big)\big]_{i,j} = \begin{cases} h_0\big(T_0(t)\big) & \text{if } i = j = 1 \\ h_E\big(T_{N+1}(t)\big) & \text{if } i = j = N+1 \\ 0 & \text{elsewhere} \end{cases}$$

With the boundary conditions relevant to our applications i.e. either rapidly changing imposed temperatures or an intense radiation source, the systems of differential equations (20) and (21) will be "stiff" (stiff problem) [32]. For such equations, the time step is limited, not for accuracy reasons, but for stability reasons. In order to overcome this constraint, very stable schemes are then used; but these are implicit and thus generally require an iterative method of resolution at each time step. In this paper, a Runge–Kutta implicit formula is used (TR-BDF2) [33].

2.2.3. Solution of the coupled system of equations

The overall solution scheme of the transient coupled equations is iterative. The flow chart of the algorithm is given in Fig. 4. First, we introduce the geometrical, thermal and radiative data, then we construct an adapted mesh.

Starting with the initial temperature field at the time $t_0 = 0$, the resolution of the RTE provides the radiation intensity field and, by integration over the angular and spectral domain, the total radiative heat flux at the time $t_0 = 0$. Taking the derivative of the total radiative heat flux with respect to the space variable, the radiative source term S_r is obtained at the time t_0. Then, the energy equation can be solved and thus the temperature field at the following time will be obtained. The iterations continue until convergence of the transient-state to the steady-state.

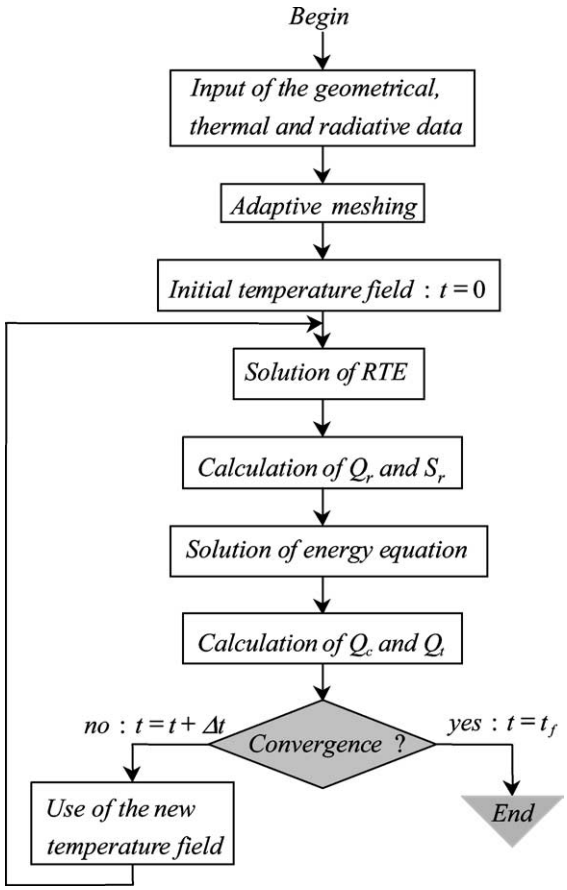

Fig. 4. Flow chart for the solution of coupled equations.

The convergence criterion for the solution of the coupled system of equations is met when the total heat flux is constant in the medium based on relation (11) or when the computed temperature behaviour satisfies the following expression:

$$\max_{1 \leqslant i \leqslant nt} \frac{|\widetilde{T}_i^{(n+1)} - \widetilde{T}_i^{(n)}|}{|\widetilde{T}_i^{(n+1)}|} < \varepsilon$$

where ε is a given strictly positive real. It is a relative termination tolerance.

In addition, a comparison on a test case, of the numerical result and the analytical solution is given in [22]. Hence, the obtained result validates the numerical method used to solve the energy equation. Moreover, we tested the stability of the method solving the coupled system of equations, by carrying out calculations with various time steps. We obtained almost the same final results.

The transient state does not change anything in the calculation of total radiative heat flux given by relation (5). Thus the steady state approximate expression given in [24] is still adequate. A discretization scheme of fourth order, using five points, is used for the approximation of the derivative. However, here, because a variable step mesh is used in the spatial domain, calculation of the radiative source term given

by (8) is not exactly the same. In this case, the calculation of the radiative source term led to the formulas given in [22].

Remark 1. The energy equation has been solved on an interval of type $[t, t + \Delta t]$ where the radiative source term is known only at the time t. Then, an approximation for this time is made, with an error of $o(\Delta t)$. Hence, it will be necessary to take a sufficiently small time step in order to minimize the error.

Remark 2. Let us note that at each time step the RTE must be solved for all the discrete wavelengths. Thus, we can expect very long computing times for the resolution of the coupled equations, especially if a transient is quite long.

3. Results and discussion

As an application of our solving method, we have treated the case of a material composed of silica fibers with a diameter of 7 microns, randomly oriented in planes parallel to the boundaries. The thickness E of the fibrous medium is equal to $E = 10$ cm. It is a material similar to those used in heat insulation. In the various applications which we will present, the same medium is studied (Fig. 3) and its radiative properties are given in Fig. 1. The glass specific heat varies little over the temperature range 300 to 500 K, so it was simpler in the modelling to suppose a constant value of $c_p = 670$ J·kg^{-1}·K^{-1} [34]. The density also remains constant in our study and is equal to $\rho = 20$ kg·m^{-3}.

As in [23,24], 12 discrete polar directions are taken with a constant angular interval and 481 wavelengths (in the range from 2 to 55 μm significant for the medium) for spectral discretization are used for the numerical solution. It was shown [3–5] that this is sufficient to obtain a correct description of the phenomena.

The calculations are performed on a Pentium IV, 1.7 Gh, 1 G RAM (PC 133) and the programs were written in FORTRAN.

In order to characterize the capability of our solving tool, the two problems studied here concern the hot guarded plates device. This is a benchmarking device for the determination of thermal characteristics of a fibrous insulator, such as the equivalent conductivity. This can be obtained by measuring the steady state heat flux through the sample placed in the hot guarded plate apparatus. Our purpose, with our transient model is to determine the time necessary to reach steady state.

3.1. Temperature boundary conditions (guarded hot plates)

We attempt to determine the time evolution of the temperature field and the heat fluxes in the medium when $T_0 = 500$ K, $T_E = 300$ K and the imposed time variation of temperature at $x = 0$ follows the law:

$$f(t) = \begin{cases} (T_0 - T_E)t + T_E, & 0 \leqslant t \leqslant 10 \text{ s} \\ T_0 \quad \text{if } t \geqslant 10 \text{ s} \end{cases}$$

We set up a non-uniform mesh, in the zone with strong temperature gradients, i.e., on the interval $[0, E/5]$, with 20 points and a discretization rule in geometric progression with a ratio $\alpha = 0.8$. The interval $[E/5, E]$ is discretized with a constant step $\Delta x = 2.5$ mm. We have used a very small time step ($\Delta t = 1s$) for stability and accuracy reasons. In these conditions, the program takes approximately 21 min. to converge, with a tolerance $\varepsilon = 10^{-6}$. Figs. 5, 6, 7 and 8 show the evolution of temperature and fluxes versus time and position in the medium. We point out that initially the temperature is constant and equal to T_E throughout the medium. At $t = 10$ s, the imposed temperatures are equal to T_0 at $x = 0$ and T_E at $x = E$. For low values of t, the material is at a temperature much lower than the black body located

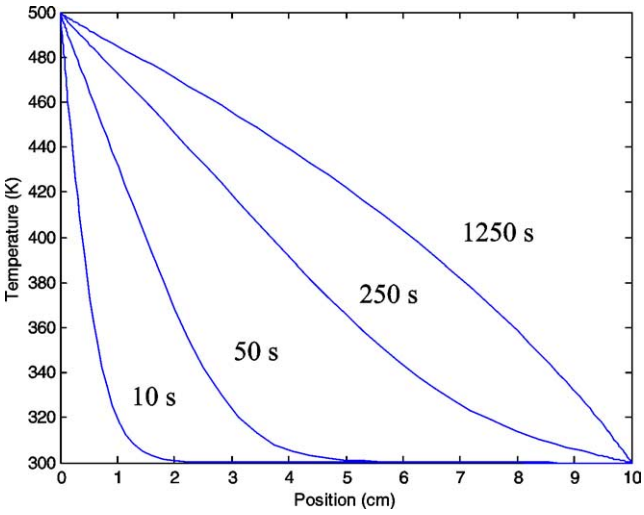

Fig. 5. Temperature at different times and positions in the medium.

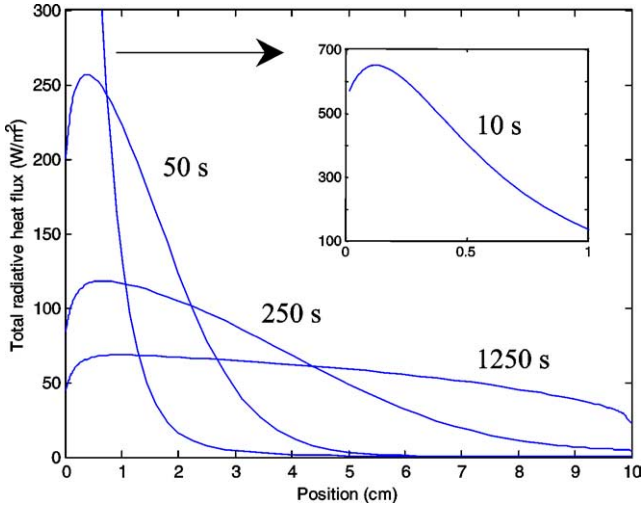

Fig. 6. Total radiative heat flux at different times and positions in the medium.

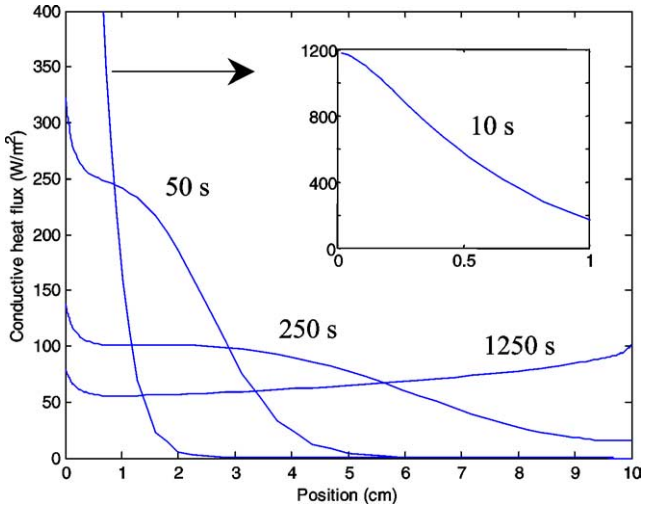

Fig. 7. Conductive heat flux at different times and positions in the medium.

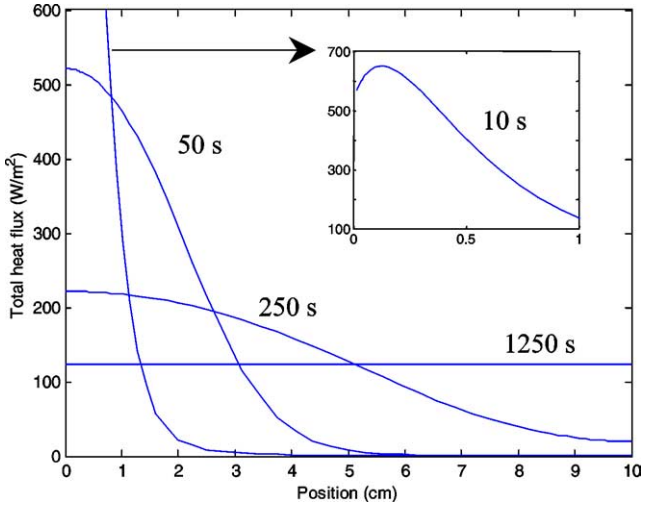

Fig. 8. Total heat flux at different times and positions in the medium.

in $x = 0$ and the temperature gradient is very significant: radiative and conductive fluxes take on very large values. The radiation and conduction coupling leads to the existence of a maximum for the radiative flux: at this point, the radiative energy source term is null. When the steady-state is reached ($t \cong 1250$ s), the total heat flux becomes constant and equal to 124 W·m^{-2}, a numerical value that we found from the previously developed steady-state model [23,24]. We also find the same value for the temperature field, the radiative and conductive fluxes. This validates the numerical method used to solve the coupled system of equations, in a transient state. In addition, with this example, the algorithm proved to be robust and stable.

3.2. Flux boundary conditions

3.2.1. Monotonously varying fluxes

For this simulation, the outer faces of the medium are exposed to the radiation emitted by blackbody sources.

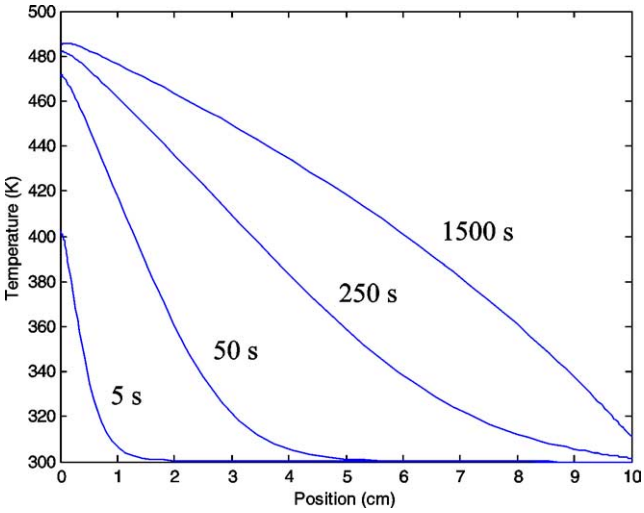

Fig. 9. Temperature at different times and positions in the medium.

On the back face ($x = E$), the source temperature is kept constant at 300 K, while on the front face ($x = 0$), the source temperature initially rises from 300 to 500 K within 1 second and then remains constant indefinitely. As to the temperature of the ambient air, in contact with the faces, it is for the sake of simplification, assumed to be: constant at 300 K on the back face ($T_{\infty,E}(t) = 300$ K) and varying, on the front face, according to the following linear evolution:

$$T_{\infty,0}(t) = \begin{cases} (150 \cdot \frac{t}{10} + 300)\ \text{K} & \text{when } 0 \leqslant t \leqslant 10\ \text{s} \\ 450\ \text{K} & \text{when } t \geqslant 10\ \text{s} \end{cases}$$

This law is arbitrarily selected.

These boundary conditions respect the axial symmetry required by our model.

For the numerical model, a spatial grid with variable step is used again; it is refined near to the two boundaries of the medium, on the two subintervals $[0, E/5]$ and $[4E/5, E]$, with 30 points for each subinterval and a discretization rule in geometric progression with a ratio $\alpha = 0.8$. The interval $[E/5, 4E/5]$ is discretized with a constant step $\Delta x = 2.5$ mm. For stability and accuracy reasons, a very small time step is used: $\Delta t = 0.5$ s. In these conditions, the program takes approximately 32 min to converge, with a tolerance $\varepsilon = 10^{-6}$. Figs. 9–12, show the evolution of the temperature fields and fluxes versus time and position in the medium. The time when the steady state is reached is approximately $t_f \cong 1500$ s. The temperature curves reach a maximum in the medium: it is the loss by convection on the front face which is responsible. In particular, that led to a conductive flux with a negative value near to the front face. The peak of radiative flux is due to the fact that the incidental flux grows very quickly: the radiation is propagated in the medium at a speed close to that of light in vacuum. The temperature rise cannot be done at the same speed, therefore the conductive flux does not vary in the same way. Fast variations of the temperature on the front face leads to a conductive flux which also strongly varies. Over approximately one quarter of the time necessary to

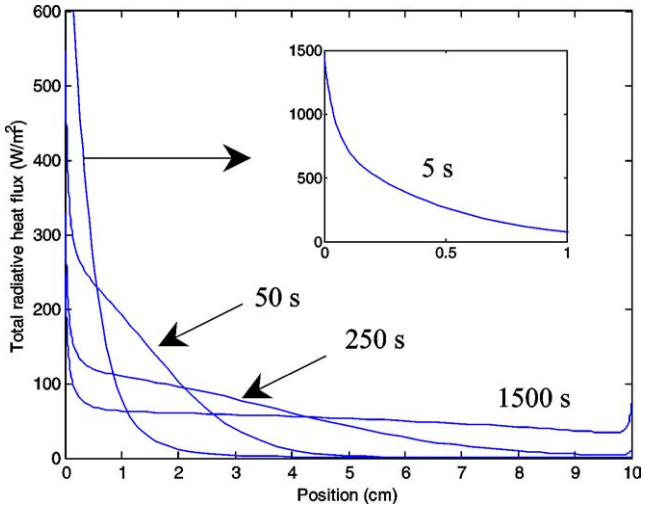

Fig. 10. Total radiative heat flux at different times and positions in the medium.

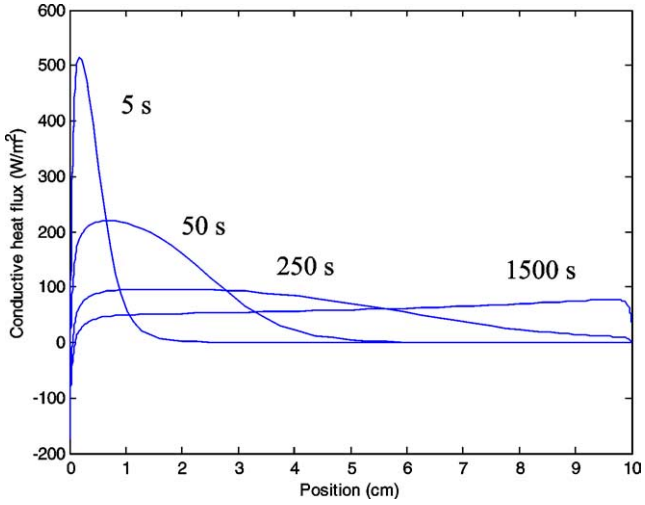

Fig. 11. Conductive heat flux at different times and positions in the medium.

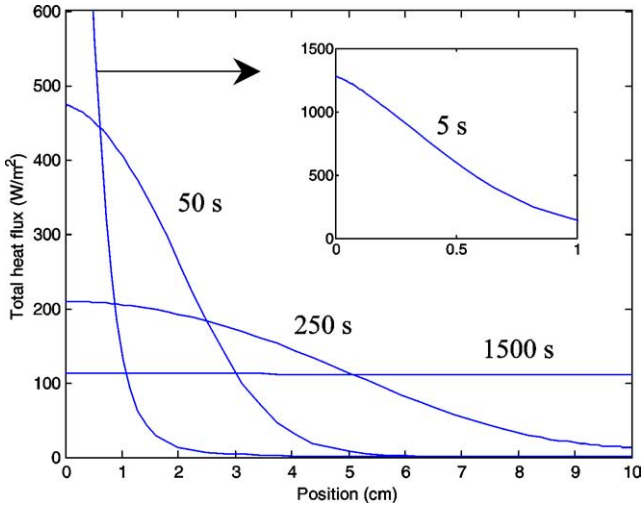

Fig. 12. Total heat flux at different times and positions in the medium.

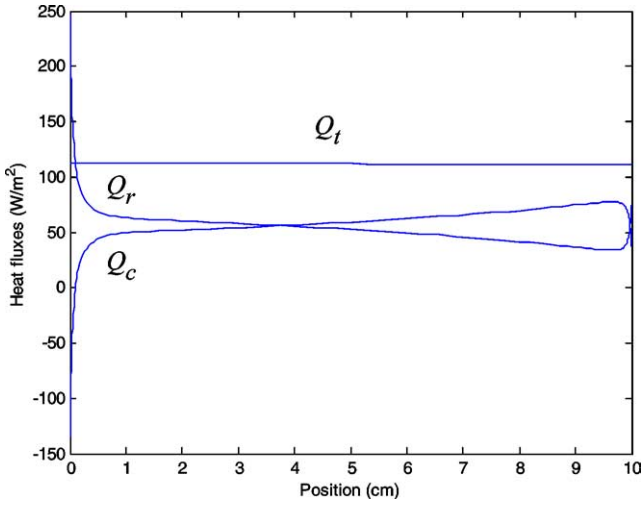

Fig. 13. Steady state heat fluxes in the medium.

reach the steady state, the temperature field is almost linear. Thus the convergence towards the steady state is much slower. When the system reaches the steady state, the total heat flux becomes constant and is equal to approximately 112 $\mathrm{W{\cdot}m^{-2}}$, with a very small relative error between the x-co-ordinates (lower than 0.6% in our case).

3.2.2. Periodically modulated fluxes

This case corresponds to the situation realized in (commercial) spectroscopic apparatuses, used for the determination of radiative properties (transmittivity, reflectivity and emissivity) of materials at room temperature: the sample is lit by an external source (such as a globar of UV lamp for infrared wavelengths), which is modulated in order to increase the sensitivity of the measurement (signal to noise ratio). Detectors are located either on the same side or on the other side of the sample with respect to the source. Accordingly, they are supposed to receive and measure either the reflected or the transmitted part of the external radiation; in any case, the internal emission of the sample is considered as negligible. Our purpose is to check the validity of this assumption in a typical situation, by evaluating, in a simulation, the (modulated) temperature field and the corresponding (modulated) emitted radiation.

The input data are similar to those detailed for the previous case, with the exception that the sample thickness is now $E = 1$ mm and the "hot" radiation source, on the front face, is at a temperature of 1000 K modulated at 10 Hz (Fig. 14). The temperature evolution on the back face has been calculated and is shown on Fig. 15: the temperature first increases for 4 seconds and then reaches a periodic regime, at a frequency equal to that of the excitation. Nevertheless, the fluctuation remains relatively weak, so that, in the case of strong radiation transmission through the sample, this small temperature change will not lead to critical errors.

In the near future, we will use our model to determine optimal experimental conditions for this spectroscopic ap-

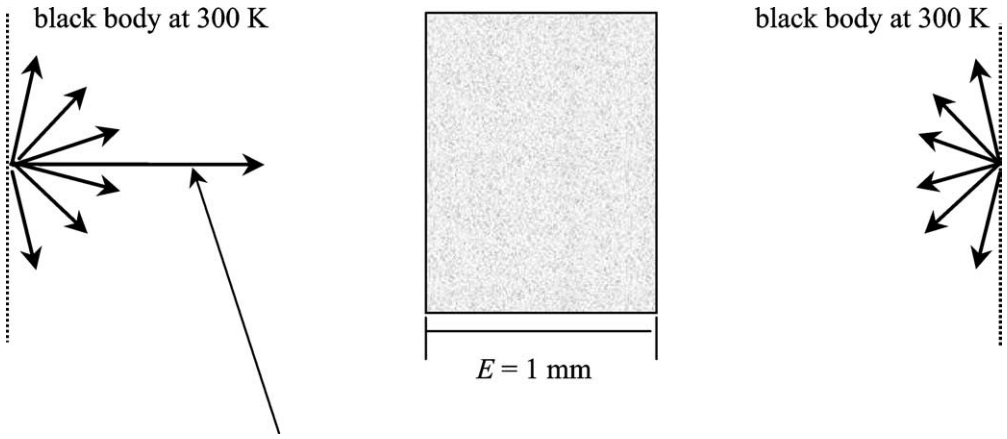

Fig. 14. Simulation scheme. Modulated part (intensity of black body at 1000 K in the normal direction with a solid angle within which the opening is equal to 15 degree), modulation frequency of 10 Hz.

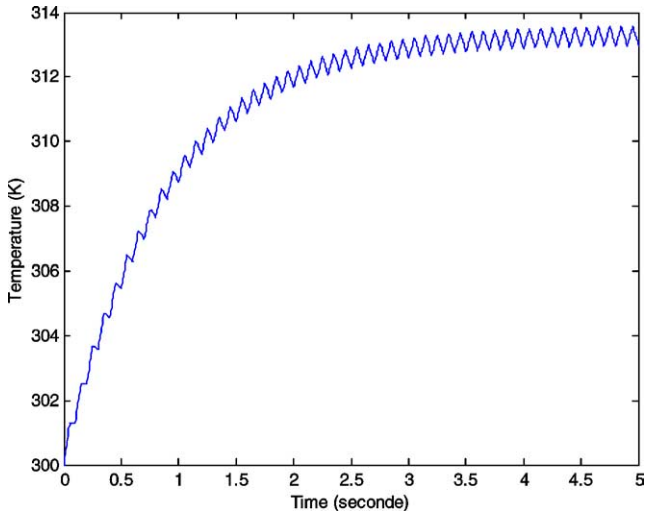

Fig. 15. Temperature rising on the back face.

paratus, or, alternatively, to evaluate the magnitude of the corrections to be applied to the measured values.

4. Conclusion

The model we have presented allows the calculation of transient radiation intensity, temperature field and heat fluxes in a fibrous medium, which may be characterised as non-grey, anisotropically absorbing, emitting and scattering, and the thermophysical properties (the conductivity and the convective exchange coefficient) which are temperature dependent. Two kinds of boundary conditions were implemented: when the temperatures imposed on the boundaries vary with time and when the medium is subjected to a radiation source which varies with time.

The numerical method used to solve the coupled system of equations is efficient (fast and very accurate). Indeed, for radiation, we use a multi-flux formulation and the numerical solution of the RTE analytical in space is fast. In addition, the Kirchhoff transformation applied to the energy equation made it possible to treat the non-linearity of the equation in a very effective and precise way. The heat fluxes and the radiative source term were calculated with high accuracy using integration and differentiation formulas of high order. The resulting equation is solved in space, by the finite element method P^2(known to be very precise) using a non-uniform mesh. The resulting differential system in time is integrated by the implicit Runge–Kutta method adapted to stiff equations. The coupling between the two equations was solved by iteration with time.

Note that the numerical method proposed here can be applied to any kind of fibrous media. This work has been validated to some extent by comparison with an experimentally confirmed steady state solution. Comparison with similar works made by other authors has not been possible because we have not found any: it seems that ours is the first published paper reporting such a complex model.

Our model has been applied to the simulation of two transient problems of practical interest. Further developments of our work will be related to the expansion of our model taking into account reflection at the wall boundary surfaces. Moreover, our numerical results will be confronted with various experimental results, in order to test the validity of our transient modelling.

Appendix A. Expressions of convective exchange coefficients

The expressions of convective exchange coefficients h_0 and h_E are approximated and determined from the Nusselt, Rayleigh, Prandtl and Grashof numbers for a vertical flat plate [35]. The Grashof number is given by the following relation:

$$G_r = \frac{g \cdot H^3}{\nu_a^2} \cdot \frac{|T - T_\infty|}{T_f}$$

where g is the gravitational acceleration, H is the height of the plate (Fig. 2), ν_a is the air cinematic viscosity, T is the

wall temperature, T_∞ is the surrounding air temperature and T_f is the air film temperature defined by $T_f = (T + T_\infty)/2$.

Calculation of the Grashof number allows determining the nature of the convective mode: if $G_r \leqslant 10^8$, the mode is laminar, otherwise the mode is turbulent. Thus, according to the mode of the air flow, one of the two following relations for the convective exchange coefficient expression is used [22]:

in laminar mode:

$$h(T) = 0.95 \cdot \frac{\lambda_{c,a}(T_f)}{\sqrt{\nu_a(T_f)}} \cdot \left(\frac{1}{H} \cdot \frac{|T - T_\infty|}{T_f}\right)^{1/4}$$

in turbulent mode:

$$h(T) = 0.25 \cdot \frac{\lambda_{c,a}(T_f)}{\nu_a(T_f)^{2/3}} \cdot \left(\frac{|T - T_\infty|}{T_f}\right)^{1/3}$$

where $\lambda_{c,a}$ is the air thermal conductivity.

These two expressions of h emphasize that they depend on variations of thermal conductivity $\lambda_{c,a}$ and cinematic viscosity ν_a with the air film temperature. From the table of the air thermodynamic properties (for a range of temperatures between 100 and 1000 K), a very approximate polynomial expression (of degree 2) of each one of these two functions is determined:

$$\lambda_{c,a}(T_f) = 10^{-4} \cdot \left(c_1 \cdot T_f^2 + c_2 \cdot T_f + c_3\right) \text{W·m}^{-1}\text{·K}^{-1}$$

with $c_1 = -2.55 \times 10^{-4}$, $c_2 = 9.2 \times 10^{-1}$, $c_3 = 6.7783$.

$$\nu_a(T_f) = 10^{-6} \cdot \left(c_4 \cdot T_f^2 + c_5 \cdot T_f + c_6\right) \text{m}^2\text{·s}^{-1}$$

with $c_4 = 7.56 \times 10^{-5}$, $c_5 = 4.76 \times 10^{-2}$, $c_6 = -4.74$.

References

[1] G. Guilbert, Etude des caractéristiques optiques des milieux poreux semi-transparents, Ph.D. Thesis, Université Henri Poincaré Nancy 1, France, 1985.

[2] G. Guilbert, G. Jeandel, G. Morlot, C. Langlais, S. Klarsfeld, Optical characteristics of semi-transparent porous media, High Temp. High Press. 19 (1987) 251–259.

[3] P. Boulet, Etude du transfert par rayonnement à travers les milieux fibreux, Ph.D. Thesis, Université Henri Poincaré Nancy 1, France, 1992.

[4] A. Milandri, Détermination des paramètres radiatifs d'un isolant fibreux: théorie de Mie, oscillateurs de Lorentz et méthode inverse, Ph.D. Thesis, Université Henri Poincaré Nancy 1, France, 2000.

[5] P. Boulet, G. Jeandel, G. Morlot, Model of radiative transfer in fibrous media-matrix method, Internat. J. Heat Mass Transfer 36 (1993) 4287–4297.

[6] G. Jeandel, P. Boulet, G. Morlot, Radiative transfer through a medium of silica fibers oriented in parallel planes, Internat. J. Heat Mass Transfer 36 (1993) 531–536.

[7] A. Milandri, F. Asllanaj, G. Jeandel, Determination of radiative properties of fibrous media by an inverse method—Comparison with the MIE theory, J. Quant. Spectrosc. Radiat. Transfer 74 (5) (2002) 637–653.

[8] D.-G. Doornink, R.-G. Hering, Transient combined conductive and radiative heat transfer, J. Heat Transfer 94 (1972) 473–478.

[9] H. Yoshida, J.-H. Yun, R. Echigo, T. Tomimura, Transient characteristics of combined conduction, convection and radiation heat transfer in porous media, Internat. J. Heat Mass Transfer 33 (5) (1990) 847–857.

[10] R. Siegel, F.-B. Molls, Finite difference solution for transient radiative cooling of a conducting semitransparent square region, Internat. J. Heat Mass Transfer 35 (10) (1992) 2579–2592.

[11] R. Siegel, Transient heat transfer in a semitransparent radiating layer with boundary convection and surface reflections, Internat. J. Heat Mass Transfer 39 (1) (1996) 69–79.

[12] C.-C. Lii, M.-N. Ozisik, Transient radiation and conduction in an absorbing, emitting, scattering slab with reflective boundaries, Internat. J. Heat Mass Transfer 15 (1972) 1175–1179.

[13] K.-C. Weston, J.-L. Hauth, Unsteady combined radiation and conduction in an absorbing, scattering and emitting medium, J. Heat Transfer 95 (1973) 357–364.

[14] T.-W. Tong, D.-L. Mcelroy, D.-W. Yarbrough, Transient conduction and radiation heat transfer in porous thermal insulations, J. Thermal Insulation 9 (1985) 13–29.

[15] C.-Y. Wu, N.-R. Ou, Transient two-dimensional radiative and conductive heat transfer in a scattering medium, Internat. J. Heat Mass Transfer 37 (17) (1994) 2675–2686.

[16] R. Siegel, Technical note: Two-flux method for transient radiative transfer in a semitransparent layer, Internat. J. Heat Mass Transfer 39 (5) (1996) 1111–1115.

[17] J.-R. Tsai, M.-N. Ozisik, Transient combined conduction and radiation in an absorbing, emitting and isotropically scattering solid sphere, J. Quant. Spectrosc. Radiat. Transfer 38 (4) (1987) 236–251.

[18] S. Andre, A. Degiovanni, A new way of solving transient radiative conductive heat transfer problems, J. Heat Transfer 120 (1998) 943–955.

[19] A.-L. Burka, Transient radiative-conductive heat transfer in a flat layer of a selective absorbing and radiating medium, J. Appl. Mech. Technical Phys. 39 (1) (1998) 91–95.

[20] O. Hahn, F. Raether, M.-C. Arduini-Schuster, J. Fricke, Transient coupled conductive/radiative heat transfer in absorbing, emitting and scattering media: Application to laser-flash measurements on ceramics materials, Internat. J. Heat Mass Transfer 40 (3) (1997) 689–698.

[21] M. Lazard, S. André, D. Maillet, Transient coupled radiative-conductive heat transfer in a gray planar medium with anisotropic scattering, J. Quant. Spectrosc. Radiat. Transfer 69 (2001) 23–33.

[22] F. Asllanaj, Etude et analyse numérique des transferts de chaleur couplés par rayonnement et conduction dans les milieux semi-transparents: Application aux milieux fibreux, Ph.D. Thesis, Université Henri Poincaré Nancy 1, France, 2001.

[23] F. Asllanaj, G. Jeandel, J.-R. Roche, Numerical solution of radiative transfer equation coupled with non-linear heat conduction equation, Internat. J. Numer. Methods Heat Fluid Flow 11 (5) (2001) 449–473.

[24] F. Asllanaj, A. Milandri, G. Jeandel, J.-R. Roche, A finite difference solution of nonlinear systems of radiative–conductive heat transfer equations, Internat. J. Numer. Meth. Engrg. 54 (2002) 1649–1668.

[25] A. Milandri, F. Asllanaj, G. Jeandel, J.-R. Roche, Heat transfer by radiation and conduction in fibrous media without axial symmetry, J. Quant. Spectrosc. Radiat. Transfer 74 (5) (2002) 585–603.

[26] M.-F. Modest, Radiative Heat Transfer, in: Mechanical Engineering Series, McGraw-Hill, New York, 1993.

[27] C. Langlais, S. Klarsfeld, Transfert de chaleur à travers les isolants fibreux en relation avec leur morphologie, J. Étude Groupement Univ. Thermique (1985) 19–53.

[28] L. Cermak, M. Zlamal, Transformation of dependent variables and the finite element solution of nonlinear evolution equations, Internat. J. Numer. Methods Engrg. 15 (1980) 31–40.

[29] J. Burger, C. Machbub, Comparison of numerical solutions of a one dimensional non-linear heat equation, Comm. Appl. Numer. Methods 7 (1991) 233–240.

[30] R.-W. Lewis, K. Morgan, H.-R. Thomas, K.-N. Seetharamu, The Finite Element Method in Heat Transfer Analysis, Wiley, New York, 1996.

[31] O.-C. Zienkiewicz, The Finite Element Method in Engineering Sciences, McGraw-Hill, New York, 1977.
[32] E. Hairer, G. Wanner, Solving Ordinary Differential Equations II. Stiff and Differential–Algebraic Problems, in: Springer Series in Computational Mathematics, Springer, New York, 1991.
[33] M.-E. Hosea, L.-F. Shampine, Analysis and implementation of TR-BDF2, Appl. Numer. Math. 20 (1996) 21–37.
[34] Y.S. Touloukian, R.K. Kirby, R.E. Taylor, et al., Thermophysical Properties of Matter, in: IFI/Plenum, vol. 13, Plenum, New York, 1972.
[35] J. Taine, J.P. Petit, Transferts thermiques mécanique des fluides anisothermes, Dunod Université, 1989.
[36] A.C. Lind, J.M. Greenberg, Electromagnetic scattering by obliquely oriented cylinders, J. Appl. Phys. 37 (8) (1986) 3195–3203.